Korean J Physiol Pharmacol 2016;20(1):119-127
http://dx.doi.org/10.4196/kjpp.2016.20.1.119

KJPP

Original Article

Comparison of electrophysiological effects of calcium channel blockers on cardiac repolarization

Hyang-Ae Lee[1,2,3], Sung-Ae Hyun[1], Sung-Gurl Park[1], Ki-Suk Kim[1,3,#,*], and Sung Joon Kim[2,#,*]

[1]Next-generation Pharmaceutical Research Center, Korea Institute of Toxicology, Daejeon 34114, [2]Department of Physiology, Seoul National University College of Medicine, Seoul 03080, [3]Human and Environmental Toxicology Program, University of Science and Technology, Daejeon 34113, Korea

ARTICLE INFO

Received October 26, 2015
Revised November 5, 2015
Accepted November 5, 2015

***Correspondence**
Ki-Suk Kim
E-mail: idkks@kitox.re.kr
Sung Joon Kim
E-mail: sjoonkim@snu.ac.kr

Key Words
Antihypertensives
Cardiac action potentials
Cardiac repolarization
Dihydropyridine calcium channel blockers
Ion channels

[#]These authors contributed equally to this work as corresponding authors.

ABSTRACT Dihydropyridine (DHP) calcium channel blockers (CCBs) have been widely used to treat of several cardiovascular diseases. An excessive shortening of action potential duration (APD) due to the reduction of Ca^{2+} channel current (I_{Ca}) might increase the risk of arrhythmia. In this study we investigated the electrophysiological effects of nicardipine (NIC), isradipine (ISR), and amlodipine (AML) on the cardiac APD in rabbit Purkinje fibers, voltage-gated K^+ channel currents (I_{Kr}, I_{Ks}) and voltage-gated Na^+ channel current (I_{Na}). The concentration-dependent inhibition of Ca^{2+} channel currents (I_{Ca}) was examined in rat cardiomyocytes; these CCBs have similar potency on I_{Ca} channel blocking with IC_{50} (the half-maximum inhibiting concentration) values of 0.142, 0.229, and 0.227 nM on NIC, ISR, and AML, respectively. However, ISR shortened both APD_{50} and APD_{90} already at 1 μM whereas NIC and AML shortened APD_{50} but not APD_{90} up to 30 μM. According to ion channel studies, NIC and AML concentration-dependently inhibited I_{Kr} and I_{Ks} while ISR had only partial inhibitory effects (<50% at 30 μM). Inhibition of I_{Na} was similarly observed in the three CCBs. Since the I_{Kr} and I_{Ks} mainly contribute to cardiac repolarization, their inhibition by NIC and AML could compensate for the AP shortening effects due to the block of I_{Ca}.

INTRODUCTION

Calcium channel blockers (CCBs) were developed in the 1970s and are now widely used for cardiovascular diseases such as hypertension and ischemic heart disease [1-4]. Since CCBs also potently inhibit Ca^{2+} influx in arterial myocytes, they induce vascular relaxation and lowering of the blood pressure. CCBs are divided into several subtypes based on their chemical structures and functional mechanisms: the dihydropyridine (DHP), phenylalkylamine and benzothiazepine classes. According to clinical guidelines, the DHP CCBs belong to the recommended first-line antihypertensive drugs to treat essential hypertension [5]. Nicardipine (NIC, first-generation), isradipine (ISR, second-generation), and amlodipine (AML, third-generation) belong to the DHP-derivative group of CCBs (Fig. 1).

On the cardiac action potential (AP), voltage-gated Na^+ channel current (I_{Na}) causes initial depolarization of upstroke phase, and thus open the voltage gated Ca^{2+} channel (VOCC) to open, allowing Ca^{2+} into the cell to prolong the AP and onto the sarcoplasmic reticular membrane to stimulate contraction through Ca^{2+}-induced Ca^{2+} release (CICR) [6]. CCBs hinder calcium entry to the cardiac myocytes, thereby reducing the amount of Ca^{2+} available to induce CICR [7].

A unique feature of cardiac AP is the plateau phase of sustained depolarization that is due to both delayed activation of voltage-gated K^+ channels currents (I_{Kv}) and VOCC current (I_{Ca}). Since the balance between I_{Ca} and I_{Kv} determines the amplitude and duration of the plateau phase of cardiac AP, pharmacological inhibition of the associated ion channels has been a critical issue of cardiac toxicity in terms of electrophysiology. I_{Kv} is composed

This is an Open Access article distributed under the terms of the Creative Commons Attribution Non-Commercial License, which permits unrestricted non-commercial use, distribution, and reproduction in any medium, provided the original work is properly cited.
Copyright © Korean J Physiol Pharmacol, pISSN 1226-4512, eISSN 2093-3827

Author contributions: H.A.L. performed patch clamp experiments and wrote the manuscript. S.A.H. performed ion channel assay. S.G.P. performed action potential assay. K.S.K. and S.J.K. supervised and coordinated the study.

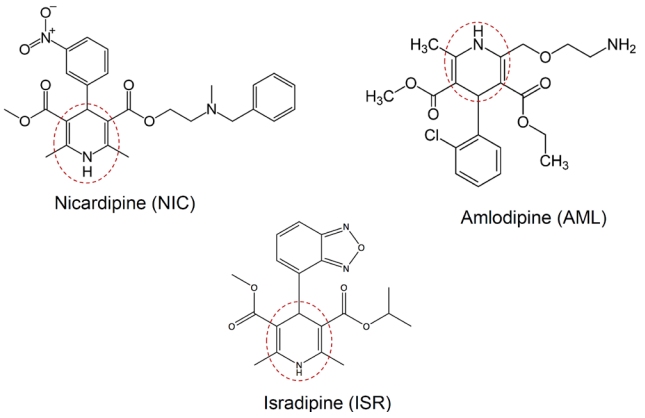

Fig. 1. Structures of dihydropyridine class-calcium channel blockers, NIC, ISR, and AML. Dihydropyridine (DHP) calcium channel blockers including NIC, ISR, and AML, are derived from the molecule dihydropyridine (red dotted circles). DHP is a molecule based upon pyridine, and the parent of a class of molecules that have been semi-saturated with two substituents replacing one double bond.

of rapidly-activating and slowly-activating voltage-gated K^+ channel currents called I_{Kr} and I_{Ks}, respectively. The inhibition of *hERG* (human ether-a-go-go-related gene) K^+ channel, the major component of I_{Kr} is the most intensively investigated target [8]. Along with the decreased *hERG* activity due to either pharmacological agents or genetic mutations, suppression of slowly-activating voltage-gated K^+ channel current (I_{Ks}) also induce the prolongation of action potential duration (APD) [9]. An abnormal APD prolongation predispose to arrhythmia due to early after-depolarization (EAD). In the heart, drug-induced QT interval prolongation in electrocardiogram (EKG) is recognized as potential risks such as torsades de pointes [10,11]. Conversely, however, less is known about short QT syndrome. Nevertheless, genetic disorders or pharmacological side effects may induce abnormally short QT intervals that could potentially increase the risk of sudden death with atrial fibrillation and/or ventricular fibrillation [12-17].

In contrast to the inhibition of K^+ channels, decreased I_{Ca} is expected to shorten APD and/or modify the shape of plateau in the cardiac AP. Therefore, CCBs can theoretically cause APD shortening. However, the above CCBs are widely used without severe side effects. Such practical safety might be due to the low plasma concentrations of CCBs in the patients prescribed with CCBs against hypertension. Another possibility is a putative compensatory inhibition of K^+ channels such as hERG, which might counterbalance the APD shortening effect of CCBs. However, precise investigations on the latter possibility is lacking yet. The purpose of this study was to examine the effects of NIC, ISR, and AML on the AP in rabbit Purkinje fibers and on cardiac ion channel currents, especially K^+ channels currents associated with the repolarization process. The integrated analysis of cardiac ion channels might provide a novel insight to understand the pharmacological effects of CCBs without critical side effects in the clinical applications.

METHODS

Animals

The experiments for AP recording and I_{Ca} analysis were performed using New Zealand white rabbit (2.5~3.5 kg) and male Sprague-Dawley (SD) rats (250~350 g), respectively. The animals were kept in a storage room under the conditions of constant temperature (23±3°C), relative humidity (50±10%), and illumination (12 h light/dark cycles) until the initiation of the experiment. This study was conducted in facilities approved by the Association for Assessment and Accreditation of Laboratory Animal Care (AAALAC) International. All procedures were approved by our Institutional Animal Care and Use Committee (IACUC).

Cell preparation

To assess the effects of CCBs on I_{Kr}, I_{Ks}, I_{K1}, and I_{Na}, HEK293 cells were transiently transfected with the following genes using Lipofectamin2000 (Gibco BRL, USA) according to the manufacturer's instructions. The *hERG* (the gene corresponding to I_{Kr}), *KCNQ1/KCNE1* (the gene corresponding to I_{Ks}), *KCNJ2* (the gene corresponding to I_{K1}) or *SCN5A* (the gene corresponding to I_{Na}) cDNA was co-transfected with green fluorescence protein (GFP) to allow assessment of the transfection efficiency. The overexpression system was adopted for the analysis of pharmacological drug effects on the above ionic currents because reliable functional isolation of respective ion channel current in cardiomyocytes is technically difficult. Although the HEK293 cells endogenously express voltage-gated K^+ currents, the peak amplitudes were less than 10% of the overexpressed I_{Kr} and I_{Ks} amplitudes.

To assess the effects of CCBs on the calcium currents, however, enzymatically isolated naïve ventricular myocytes were used because consistent co-expression of multilple subunits of L-type Ca^{2+} channel proteins were requested. Briefly, the hearts were rapidly excised from anesthetized SD rats and perfused via the aorta on a Langendorff apparatus with an oxygenated normal Tyrode's (NT) solution for 5 min to clear the blood, then perfused with Ca^{2+}-free NT solution for 3 min. Next the heart was perfused with enzyme solution containing 0.6 mg/ml collagenase (Worthington, type 2, USA) for 30~40 min. Finally, this enzyme-containing solution was washed out for 5 min with a high-K^+ and low-Cl^- Kraft-Bruhe (KB) solution. Following the isolation procedure, the left ventricle was dissected out and agitated mechanically with a fire-polished Pasteur pipette in KB solution to obtain single myocytes. The isolated myocytes were stored at 4°C until use for up to 8 hour.

Drugs and Solutions

NIC, ISR and AML were purchased on Sigma-aldrich (MO, USA). These were formulated into stock solution with dimethyl sulfoxide (DMSO). All the drug stock solutions were diluted in normal Tyrode (NT) solution to produce the target exposure concentrations. The concentration of DMSO in NT was always kept 0.1%. The external solution for recording the I_{Kr}, I_{Ks} and I_{Na} was NT solution as follows (in mM): 143 NaCl, 5.4 KCl, 1.8 $CaCl_2$, 0.5 $MgCl_2$, 5 HEPES, 0.33 NaH_2PO_4 and 16.6 glucose (pH adjusted to 7.4 with NaOH).

The internal solution for recording I_{Kr} contained the following (in mM): 130 KCl, 5 Ethylene glycol-bis(2-aminoethylether)-N,N,N',N'-tetraacetic acid (EGTA), 10 4-(2-hydroxyethyl) piperazine-1-ethanesulfonic acid (HEPES), 1 $MgCl_2$, and 5 Mg-ATP (pH adjusted 7.25 with KOH). For recording I_{Ks} the internal solution contained (in mM) 150 KCl, 5 EGTA, 10 HEPES, 2 $MgCl_2$, 1 $CaCl_2$ and 5 Na_2-ATP (pH adjusted 7.25 with KOH). For recording I_{K1}, the internal solution contained (in mM) : 130 K-Asp, 15 KCl, 10 HEPES, 1 $MgCl_2$, 5 Na_2-ATP, 5 EGTA (pH adjusted 7.25 with KOH). For recording I_{Na}, the internal solution contained 105 CsF, 35 NaCl, 10 EGTA, 10 HEPES (pH adjusted to 7.25 with NaOH).

For recording I_{Ca}, the fresh isolated rat ventricular myocytes were superperfused with an external solution that consisted of (in mM): 137 cholin-Cl, 5 CsCl, 0.5 $MgCl_2$, 2 4-AP, 10 HEPES, 10 glucose and 1.8 $CaCl_2$ (pH adjusted to 7.4 with NaOH). The internal solution for I_{Ca} recording contained (in mM): 20 CsCl, 100 Cs-aspartate, 10 EGTA, 10 HEPES, 20 Tetraethylammonium chloride (TEA-Cl), 5 Mg-ATP (pH adjusted to 7.25 with KOH). KB solution for storage of the freshly isolated rat ventricular myocytes contained (in mM): 70 K-glutamate, 55 KCl, 10 HEPES, 3 $MgCl_2$, 20 taurine, 20 KH_2PO_4, 0.5 EGTA (adjusted to pH 7.2 with KOH).

Recording of action potentials on rabbit Purkinje fibers

The rabbits were anesthetized with pentobarbitone sodium (30~50 mg/kg i.v.) and then their hearts were rapidly removed and placed in oxygenated NT solution to pump the remaining blood out. The left ventricle was opened and Purkinje fibers were carefully dissected out with a small piece of ventricular tissue to be pinned in the experimental chamber. The isolated Purkinje fibers were superfused with oxygenated NT solution (5 ml/min) maintained at 37.0±0.5°C. The preparations were electrically stimulated at a basal rate (frequency=1 Hz, duration=2 ms, voltage=1.5~2 V). Two hours were allowed for each preparation to equilibrate while continuously superfused with NT solution. Action potentials were recorded using the conventional intracellular recording technique involving a glass microelectrode filled with 3 M KCl and connected to a Geneclamp 500B (Axon Instruments, CA, USA). Action potential duration at 50% and 90% repolarization (APD_{50} and APD_{90}) was automatically measured using Notocord HEM program (NOTOCORD, France) at a sampling rate of 50 kHz. Before drug treatment, action potential parameters were measured in NT for 1 hour to establish stable control value recording. The vehicle control (0.01% DMSO in NT) and drugs were perfused every 20 min after the stable AP were obtained. Besides AP, resting membrane potential (RMP), total amplitude (TA), and maximum velocity of initial depolarization (Vmax) were analyzed (Table 1). The RMP values in the Purkinje fibers usually lie between –89 and –72 mV. The tested fibers were randomly allocated to each test agent. However, since the numbers of tested tissues are not large, accidental gathering of relatively hyperpolarized Purkinje fibers for a specific test group could results in an outlier-like data (see the RMP for the ISR group in Table 1).

Recording of ionic currents

The cells were placed in a recording chamber on the stage of a Nikon inverted microscope, and continuously perfused (5±1 ml/min) with 37±1°C bath solution. Ionic currents were recorded in a whole-cell configuration with a standard patch clamp technique using a HEKA EPC8 amplifier (Electronik, Lambrecht, Germany). Data were recorded during the approximately 5 minutes following initial application of the bath solution to verify currents stability. Test drug solutions were subsequently superfused for approximately 5 minutes to achieve steady-state blocks. To investigate the effect of these drugs on the ion channel currents, various concentrations (0.01~30 μM) of drugs were tested. Voltage-clamp protocol generation and data acquisition were controlled by computers equipped with an A/D converter, Digidata (Axon Inc., USA) and RClamp software developed by Seoul National University (Seoul, Korea). The patch pipettes were made from borosilicate glass capillaries (Clark Electromedical Instruments, UK) using a pipette puller (PP-830, Narishige, Japan). Their resistances were 3~4 MΩ when filled with pipette solution. The current signals were filtered at a sampling rate of 5 kHz, and they were low-pass filtered at 1 kHz and stored on computer. All experimental parameters, such as pulse generation and data acquisition, were controlled using the RClamp software.

Statistical Methods

Data analysis and curve fitting of patch clamp experiments were carried out using RClamp, GraphPad InStat (GraphPad Software, San Diego, CA), and SigmaPlot 2000 (SPSS Inc., Chicago, IL). Pooled data are expressed as means±standard errors of the mean (SEM), and statistical comparisons were made with $p<0.05$, or $p<0.01$ considered significant. Current amplitudes were measured before and after application of the respective drugs. The percent inhibition values were calculated according to

Table 1. Effects of CCBs on the electrical parameters of rabbit Purkinje fibers

	Concentration	RMP (mV)	Vmax (v/s)	TA (mV)
NIC	0	–76.00±1.97	509.05±88.96	114.19±4.67
	10 nM	–76.22±3.91	416.09±52.63	111.82±3.64
	300 nM	–77.25±4.77	448.73±60.92	113.41±2.91
	1 μM	–78.19±5.71	468.54±40.15	113.78±2.32
	30 μM	–77.95±7.99	374.32±28.49	112.46±1.66
ISR	0	–86.37±2.50	276.34±24.15	113.38±3.49
	10 nM	–86.27±3.47	263.67±25.67	113.41±2.91
	300 nM	–81.81±0.73	273.69±29.03	113.48±4.36
	1 μM	–80.47±0.79	241.91±18.79	110.87±3.90
	30 μM	–75.84±0.95*	150.37±29.64*	104.16±4.45
AML	0	–80.10±1.61	426.90±101.04	118.98±0.51
	10 nM	–79.98±1.42	421.50±94.01	118.30±1.00
	300 nM	–79.87±1.48	419.22±92.76	118.09±1.23
	1 μM	–78.05±2.22	375.63±57.63	113.98±3.36
	30 μM	–75.83±1.51	330.72±68.77	108.91±0.94**

Data are expressed as mean±SEM of 4 rabbits in each drug. The data were analyzed for homogeneity of variance using Bartlett's test. Homogeneous data were analyzed using the Analysis of Variance and the significance of inter-group differences between each dose groups and the vehicle-control group were assessed using Dunnett's test. Heterogeneous data were analyzed using Kruskal-Wallis test and the significance of inter-group differences between the control and test article groups were assessed using Dunn's Rank Sum test. Statistical analyses were performed by using Statistical Analysis Systems (SAS/STAT Version 9.2, Cary, USA). RMP, resting membrane potential; Vmax, maximal upstroke velocity of phase 0; TA, total amplitude. *p<0.05, **p<0.01.

the following equation:

$$\%\text{inhibition} = \frac{\text{Initial current amplitude (control) - Current amplitude in the presence of drug}}{\text{Initial current amplitude (control)}} \times 100$$

Effects were calculated from the results of 3~5 experiments per concentration of the drugs. Concentration response relations were calculated by a non-linear least squares fit equation [Hill equation; $f=x^H/(IC50^H+x^H)$; H=Hill coefficient, IC50=IC_{50}, x=concentration, f=inhibition ratio] using the SigmaPlot 2000 program for the half-maximum inhibiting concentration (IC_{50}).

RESULTS

Effects of CCBs on I_{Ca} and I_{Na}

We first examined their inhibitory potency for Ca^{2+} channel currents in rat ventricular myocytes. The I_{Ca} was activated by a depolarizing step pulse (0 mV, 500 ms) from the holding potential of –80 mV (Fig. 2A). All three CCBs inhibited the I_{Ca} in a concentration-dependent manner (Fig. 2A). NIC at 0.01, 0.1, 1, and 10 μM reduced the I_{Ca} amplitude by 18.4%, 41.5%, 78.3%, and 99.4%, respectively (n=3). ISR at the same concentrations attenuated the I_{Ca} amplitude by –3.2%, 22.6%, 89.9%, and 99.8%, respectively (n=3). In addition, AML also had potent inhibitory effect on I_{Ca}. AML reduced the I_{Ca} amplitude by 13.8%, 34%, 72.5%, and 100% at 0.01, 0.1, 1, and 10 μM, respectively (n=3). The IC_{50} values were 0.142±0.03 μM for NIC, 0.227±0.28 μM for ISR, and 0.229±0.02 μM for AML (Fig. 2B).

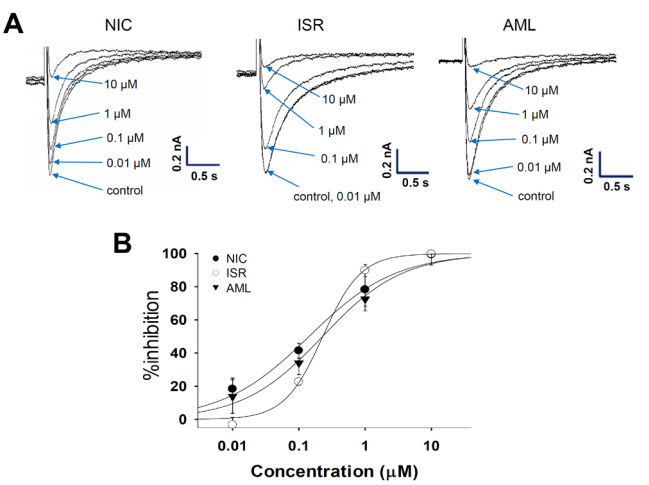

Fig. 2. Effect of NIC, ISR, and AML on I_{Ca} in rat cardiomyocytes. (A) I_{Ca} traces of rat cardiomyocytes under before and after application of 0.01, 0.1, 1, and 10 μM of CCBs. (B) Concentration response curves for inhibition of I_{Ca} by the CCBs, providing the IC_{50} values of 0.142±0.03 μM for NIC, 0.227±0.28 μM for ISR, and 0.229±0.02 μM for AML (each n=3).

In *SCN5A* overexpressed cells, I_{Na} was generated by a step pulse from –100 mV of holding voltage to –40 mV of 20 ms duration. The CCBs also inhibited I_{Na} at micromolar ranges (Fig. 3A). 30 μM ISR almost completely inhibited I_{Na} while NIC and AML inhibited I_{Na} by about 80% at 30 μM. When fitted to a Hill function, their IC_{50} values were 7.08, 3.05, and 6.38 μM for NIC, ISR, AML, respectively (n=4, Fig. 3B).

 http://dx.doi.org/10.4196/kjpp.2016.20.1.119

Effects of CCBs on the cardiac APs in rabbit Purkinje fibers

ICH S7B guideline S7B recommends an integrated approach for cardiovascular preclinical evaluation of new drug candidates, including action potential assays with isolated cardiac tissues from guinea pig, rabbit, and canine to predict the potential of drugs to induce abnormal cardiac events. Among them, the AP assay using rabbit Purkinje fibers was considered a valuable assay for evaluating the proarrhythmic pharmaceuticals as it can reveal complex electrophysiological profiles that modulate repolarization delay [18]. To evaluate the integrated electrophysiological effects of CCBs, we performed rabbit Purkinje fiber assay with these CCBs.

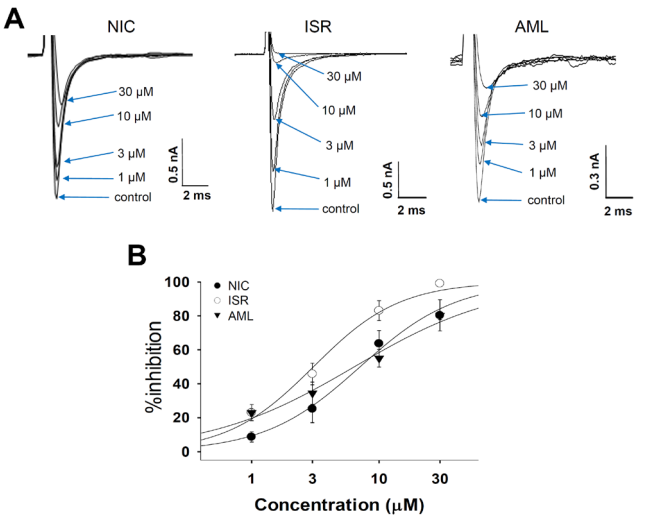

Fig. 3. Effect of NIC, ISR, and AML on I_{Na} in HEK293. (A) Representative I_{Na} traces under control conditions and after application of various test concentrations of NIC, ISR, and AML. (B) Statistical summary and Hill's fitting of concentration–dependent inhibitions of I_{Na} for these drugs (each n=4). It provided the IC_{50} values of approximately 7.08, 3.05, and 6.38 μM for NIC, ISR, AML, respectively.

Fig. 4 shows the concentration-dependent effects of NIC, ISR and AML on the APs in rabbit Purkinje fibers. NIC at a concentration of 30 μM induced a triangulated AP and significantly shortened the APD_{50} compared vehicle control by –69 ms±9.9 while not affecting APD_{90} (n=4, p<0.05, Fig. 3A and 3D). The other AP parameters, including resting membrane potential (RMP), maximum velocity of initial depolarization in the phase 0 (V_{max}) and the total amplitude (TA) were not changed (Table 1). AML at 30 μM also significantly shortened the APD_{50} by –58.3 ms±9.3 (n=4, p<0.01, Fig. 4C and 4F) while not significantly decreased the APD_{90}. AML also decreased TA by –10 mV±0.93 (Table 1). NIC and AML induced a triangulated shape of AP (Fig. 4A and 4C). Unlike NIC and AML, ISR at 30 μM significantly shortened both the APD_{50} and APD_{90} by –88.5 ms±7.3 and –82.9 ms±8.8, respectively (n=4, p<0.01). ISR at 1 μM also markedly shortened the APD_{90} by –40 ms±17.8 (p<0.05, n=4, Fig. 4B and 4E). In addition, ISR at 30 μM significantly decreased the RMP (–10.5 mV±3.4, p<0.05) and V_{max} (–126 V/s±10, p<0.05), but had no significant effect on the TA (Table 1).

Effects of CCBs on repolarizing K^+ currents

To examine the tail components of I_{Kr} which reflect the repolarizing K^+ current in the cardiac AP, the cells were depolarized for 2 s to +20 mV from a holding potential of –80 mV followed by a 3s repolarization back to –40 mV. Fig. 4A shows the representative cases of the voltage-clamp recording from *hERG*-transfected HEK293 cells. NIC and AML commonly inhibited I_{Kr} in a concentration-dependent manner, and almost complete inhibition was observed at 30 μM (Fig. 5A and 5B). NIC at concentrations of 0.1, 0.3, 1, and 3 μM reduced the I_{Kr} amplitude by

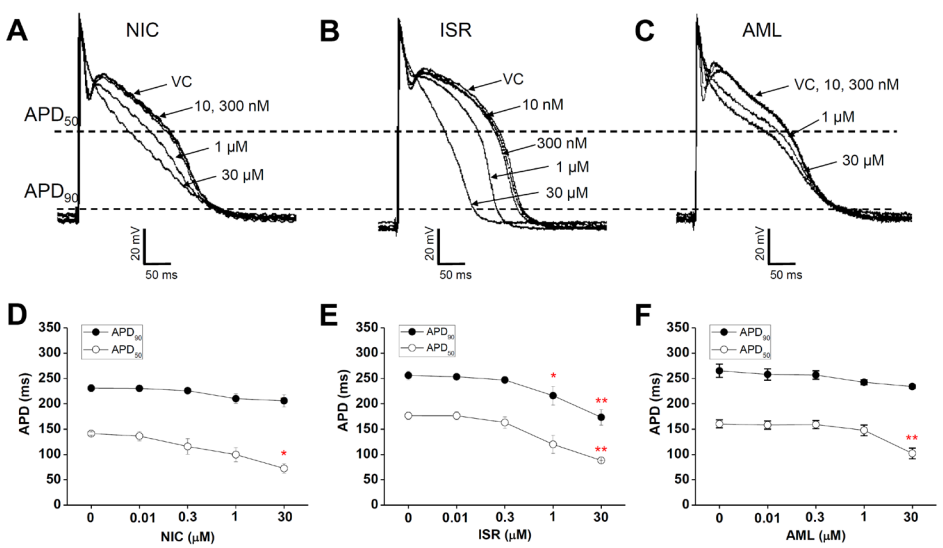

Fig. 4. Concentration-dependent effects of NIC, ISR and AML on the AP in rabbit Purkinje fibers. (A~C) Representative illustrations for the effects of NIC, ISR, and AML on the cardiac AP in rabbit Purkinje fibers. (D~F) Effects of NIC , ISR, and AML on the action potential duration of rabbit Purkinje fibers at 50% (APD_{50}, opened circles) and 90% repolarization (APD_{90}, closed circles). Data are expressed as mean±SEM and compared by ANOVA followed by Dunnett's test (each n=4). *p<0.05; **p<0.01, compared with VC (vehicle control, 0.1% DMSO in NT).

5.1±2.9%, 13.0±2.5%, 40.1±5.5%, and 83.0±7.3%, respectively (n=4). AML at the same concentrations inhibited the I_{Kr} amplitude by 5.2±2.9%, 17.5±3.3%, 67.6±4.0%, and 90.4±5.1%, respectively (n=4). However, ISR at 1, 3, 10, and 30 μM inhibited the I_{Kr} amplitude by 2.6±1.6%, 15.6±7.7%, 26.0±7.3%, and 42.2±6.6%, respectively (n=4). The Hill equation fitting function was applied and IC_{50} values were measured to examine the relative potency of I_{Kr} inhibition (Fig. 5B). The IC_{50} values were 0.88±0.05 μM for NIC and 6.78±0.36 μM for AML. Since the maximum inhibition rate of ISR was smaller than 50%, we could

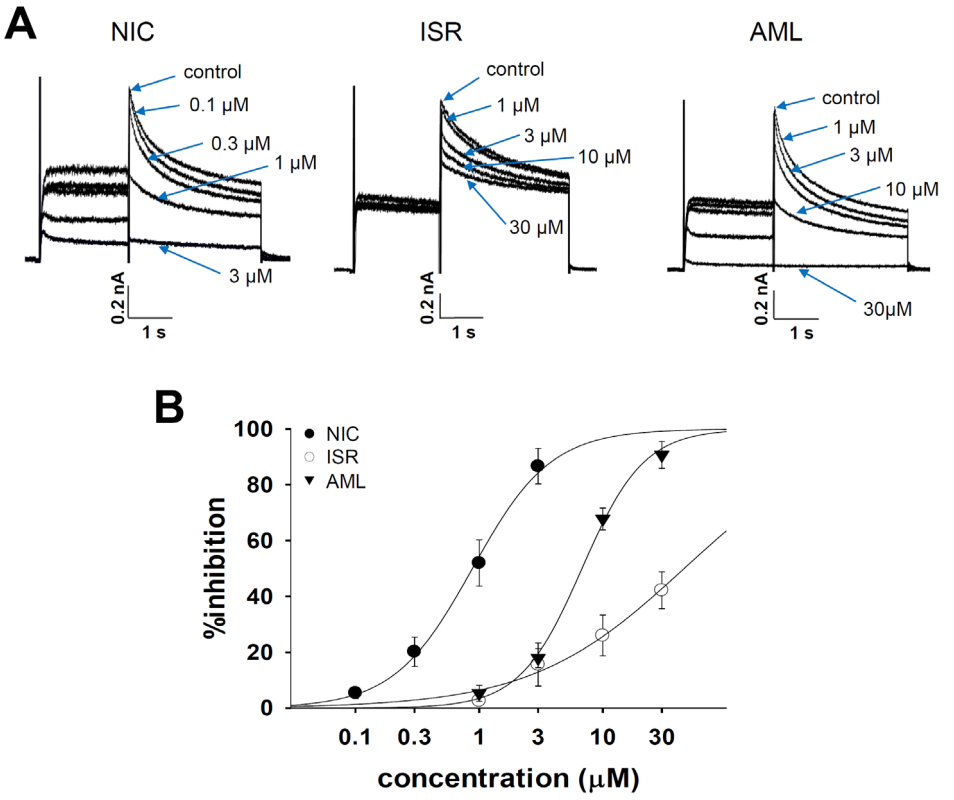

Fig. 5. Effect of NIC, ISR and AML on I_{Kr} in HEK293 cells. (A) Representative current traces of I_{Kr} under control and after application of various concentrations ranging from 0.1~30 μM of NIC, ISR, and AML. (B) Concentration–dependent inhibitions of I_{Kr} for NIC, ISR, and AML were summarized and fitted with Hill function (each n=4). The IC_{50} values were 0.88±0.05 μM for NIC, 6.78±0.36 μM for AML, and >30 μM for ISR.

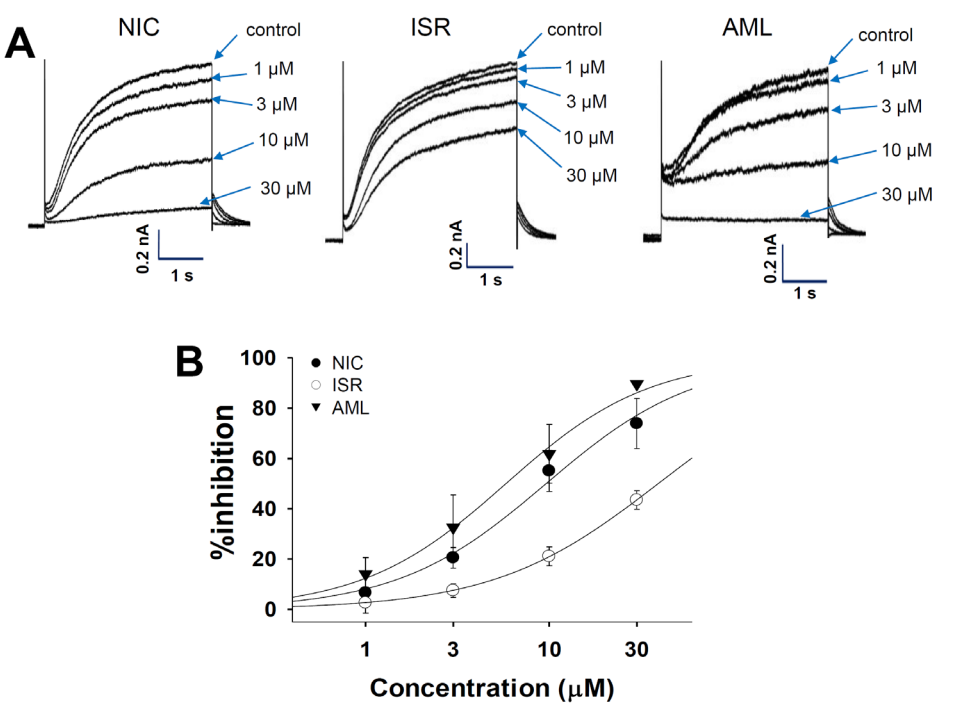

Fig. 6. Effect of NIC, ISR and AML on I_{Ks} expressed in HEK293 cells. (A) Representative current traces showing the effects of NIC, ISR, and AML on I_{Ks} at doses of 1, 3, 10, and 30 μM, respectively. (B) Dose-response relationships of I_{Ks} for NIC, ISR, and AML were summarized and fitted with Hill function (each n=4).

http://dx.doi.org/10.4196/kjpp.2016.20.1.119

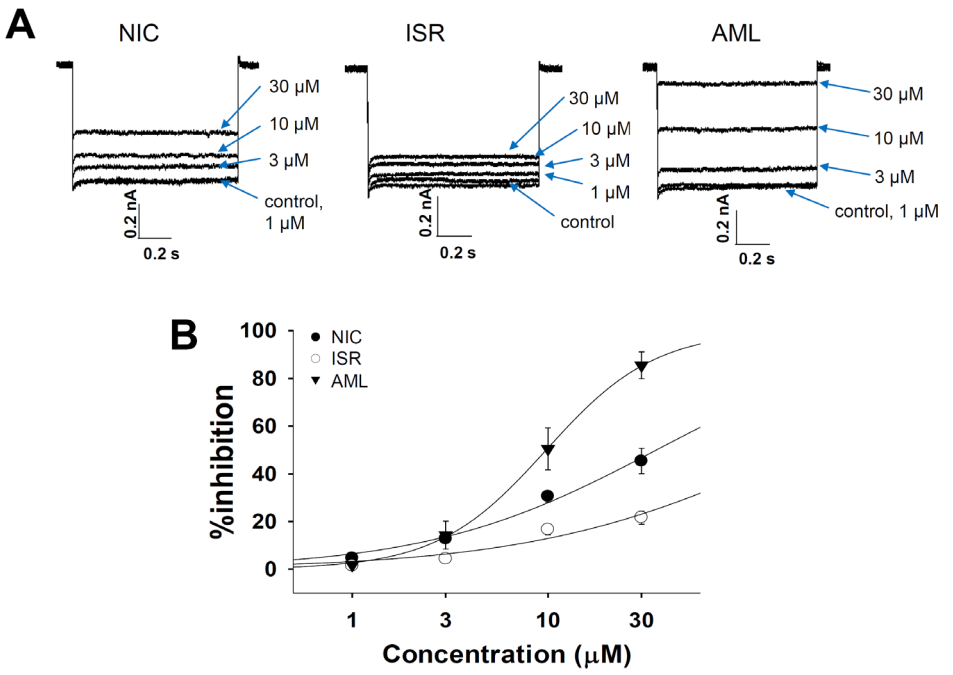

Fig. 7. Effect of NIC, ISR and AML on I_{K1} expressed in HEK293 cells. (A) Representative current traces demonstrating the effects of NIC, ISR, AML on I_{K1} at 0 (control), 1, 3, 10, 30 μM, respectively. (B) Concentration–dependent inhibitions of I_{K1} induced by NIC, ISR, and AML were summarized and fitted with Hill function for IC_{50} values (each n=4). The IC_{50} value of AML on the I_{K1} was 9.78±0.18 μM. Since the maximum inhibition rates of NIC and ISR were smaller than 50%, we could not obtain the IC_{50} values for these drugs.

not obtain the IC_{50} value for ISR.

For recording I_{Ks}, the KCNQ1/KCNE1-coexpressing cells were depolarized for 3 s to +60 mV from a holding potential of −80 mV, followed by a 3s repolarization back to −40 mV. Fig. 6A shows the representative current traces under control conditions and after exposure to 1, 3, 10, and 30 μM NIC, ISR, and AML. Similar to the effects on I_{Kr}, NIC and AML inhibited the I_{Ks} in a concentration-dependent manner while ISR incompletely inhibited I_{Ks} even at 30 μM. Fig. 6B shows the concentration-response curves for these drugs. The IC_{50} values were approximately 9.61±1.01 μM for NIC and 5.81±0.5 μM for AML. Since the maximum inhibition rate of ISR was smaller than 50%, we could not obtain the IC_{50} value for ISR.

Fig. 7A shows the represented currents traces from *KCNJ2*-transfected HEK293 cells and the effects of CCBs. The I_{K1} was elicited by a hyperpolarizing step pulse from −80 mV to −120 mV of 1 s duration. All of the three drugs inhibited the I_{K1} in a concentration-dependent manner, however, the maximum inhibition rates of NIC and ISR at 30 μM were below 50% (45.4±5.3%, and 21.7±2.8%, respectively, each n=4). The IC_{50} value of AML on the I_{K1} was 9.78±0.18 μM (Fig. 7B, n=4).

DISCUSSION

Here we evaluated the electrophysiological safety of the most commonly used DHP class of CCBs by assessing their effects on the ion channel currents involved in cardiac APD and on repolarization phase in rabbit Purkinje fibers. Despite the common inhibitory effects on I_{Ca}, the APD shortening was not consistent between the three CCBs tested here. APD_{90} was significantly decreased only by ISR from 1 μM whereas APD_{50} was commonly decreased by NIC, ISR and AML at 30 μM. As a result, the AP was generally shortened by ISR whereas showed triangulation in response to NIC and AML. In addition to the above findings, ISR at 30 μM decreased the RMP and V_{max} while not the TA (Table 1). The decrease of V_{max} might be due to the more potent inhibition of I_{Na} by ISR than by NIC and AML (Fig. 3).

Except ISR, relatively high concentrations of NIC and AML were required to significantly decrease the APD_{90} of rabbit Purkinje fibers. Indeed, the present ICH S7B guideline [19] does not specifically address the possibility of a drug-induced shortening of the QT interval. Although the QT-shortening could potentially increase the ventricular tachycardia and the ventricular fibrillation risk of sudden death [20-24], Roden [25] and Hondeghem [26,27] have suggested that simple QT interval change is a poor marker for proarrythmic susceptibility. However, many experiments in isolated rabbit hearts demonstrated that triangulation (prolongation of the fast repolarization phase) is proarrhythmic [26] that was confirmed by other groups [28-31]. Triangulation may be accompanied by either shorting or lengthening of the total action potential duration. In this study, NIC and AML induced the triangulation of AP. However, relatively high concentration (e.g. 30 μM) was required to reveal the triangulation of AP, suggesting the safety of CCBs.

Several large clinical trials that have consistently shown that no significant increase in sudden cardiac death with DHP class of CCBs even in vulnerable patients [32-35]. In fact, the reported plasma concentrations of NIC, ISR and AML ranges below micromolar concentrations [36-38] where no significant changes in APD were observed with NIC and AML in the present study. The DHP calcium channel modulators do not exert significant

electrophysiologic effects on the myocardium and specialized conduction tissue at clinically relevant doses that dilate vascular smooth muscle *in vivo*. Owing to the relative selectivity of CCBs on vascular smooth muscle, significant depressant effects on myocardial contractility and atrioventricular conduction could be avoided [39]. However, the tissue-dependent selectivity can be lost in overdose situations [40]. In this respect, the potent inhibition of I_{Ca} without significant APD shortening by NIC and AML observed in the present study might imply an additional safety mechanism besides the plasma concentrations.

Here we suggest that the lack of actual clinical problems might be due, at least partly, to the concomitant changes in other ion channel activities. In addition to the inhibition of I_{Ca}, NIC and AML showed concentration-dependent inhibition of I_{Kr} and I_{Ks}; (Fig. 5 and 6). The inhibitory effects of ISR on I_{Kr} and I_{Ks} were incomplete (<50% at 30 μM). Since the voltage-gated K^+ channels would mainly contribute to cardiac repolarization, their inhibition by NIC and AML might compensate for the putative APD shortening effects of these CCBs.

In summary, despite the potent I_{Ca} inhibition, NIC and AML do not induce a significant shortening of APD up to 30 μM of applied concentration. According to ion channel studies, concomitant inhibition of I_{Kr} and I_{Ks} might differentially counterbalance the influence to cardiac repolarization of CCBs. Further investigation of other classes of CCBs' effects on the cardiac K^+ channel currents are requested for the integrative understanding of cardiac toxicity. Such study could include the physiological components having multiple effects on cardiac functions including ion channels [41]. Finally, our present study gives a message that the integrative analyses of various ion channel currents could provide a novel insight for the pharmacological effect as well as the safety for the clinical applications of drug compounds under development [42].

ACKNOWLEDGEMENT

This research was supported by the Bio & Medical Technology Development Program of the National Research Foundation (NRF) funded by the Ministry of Science, ICT & Future Planning (MSIP), Republic of Korea (No. NRF-2012M3A9C7050138).

REFERENCES

1. Dahlöf B, Sever PS, Poulter NR, Wedel H, Beevers DG, Caulfield M, Collins R, Kjeldsen SE, Kristinsson A, McInnes GT, Mehlsen J, Nieminen M, O'Brien E, Ostergren J; ASCOT Investigators. Prevention of cardiovascular events with an antihypertensive regimen of amlodipine adding perindopril as required versus atenolol adding bendroflumethiazide as required, in the Anglo-Scandinavian Cardiac Outcomes Trial-Blood Pressure Lowering Arm (ASCOT-BPLA): a multicentre randomised controlled trial. *Lancet*. 2005; 366:895-906.
2. Siragy HM. Major outcomes in high-risk hypertensive patients randomized to angiotensin-converting enzyme inhibitors or calcium channel blocker vs diuretic. The Antihypertensive and Lipid-Lowering Treatment to Prevent Heart Attack Trial (ALLHAT). *Curr Hypertens Rep*. 2003;5:293-294.
3. Black HR, Elliott WJ, Grandits G, Grambsch P, Lucente T, White WB, Neaton JD, Grimm RH Jr, Hansson L, Lacourciere Y, Muller J, Sleight P, Weber MA, Williams G, Wittes J, Zanchetti A, Anders RJ; CONVINCE Research Group. Principal results of the Controlled Onset Verapamil Investigation of Cardiovascular End Points (CONVINCE) trial. *JAMA*. 2003;289:2073-2082.
4. Pepine CJ, Handberg EM, Cooper-DeHoff RM, Marks RG, Kowey P, Messerli FH, Mancia G, Cangiano JL, Garcia-Barreto D, Keltai M, Erdine S, Bristol HA, Kolb HR, Bakris GL, Cohen JD, Parmley WW; INVEST Investigators. A calcium antagonist vs a non-calcium antagonist hypertension treatment strategy for patients with coronary artery disease. The International Verapamil-Trandolapril Study (INVEST): a randomized controlled trial. *JAMA*. 2003;290: 2805-2816.
5. Burnier M, Pruijm M, Wuerzner G. Treatment of essential hypertension with calcium channel blockers: what is the place of lercanidipine? *Expert Opin Drug Metab Toxicol*. 2009;5:981-987.
6. Hirano Y, Hiraoka M. Electrophysiology of cardiac ion channels. *Nihon Rinsho*. 1996;54:2050-2055.
7. DeWitt CR, Waksman JC. Pharmacology, pathophysiology and management of calcium channel blocker and beta-blocker toxicity. *Toxicol Rev*. 2004;23:223-238.
8. Priest BT, Bell IM, Garcia ML. Role of hERG potassium channel assays in drug development. *Channels (Austin)*. 2008;2:87-93.
9. Barhanin J, Attali B, Lazdunski M. IKs, a slow and intriguing cardiac K^+ channel and its associated long QT diseases. *Trends Cardiovasc Med*. 1998;8:207-214.
10. Haverkamp W, Breithardt G, Camm AJ, Janse MJ, Rosen MR, Antzelevitch C, Escande D, Franz M, Malik M, Moss A, Shah R. The potential for QT prolongation and proarrhythmia by non-antiarrhythmic drugs: clinical and regulatory implications. Report on a policy conference of the European Society of Cardiology. *Eur Heart J*. 2000;21:1216-1231.
11. Cubeddu LX. QT prolongation and fatal arrhythmias: a review of clinical implications and effects of drugs. *Am J Ther*. 2003;10:452-457.
12. Gaita F, Giustetto C, Bianchi F, Wolpert C, Schimpf R, Riccardi R, Grossi S, Richiardi E, Borggrefe M. Short QT Syndrome: a familial cause of sudden death. *Circulation*. 2003;108:965-970.
13. Giustetto C, Di Monte F, Wolpert C, Borggrefe M, Schimpf R, Sbragia P, Leone G, Maury P, Anttonen O, Haissaguerre M, Gaita F. Short QT syndrome: clinical findings and diagnostic-therapeutic implications. *Eur Heart J*. 2006;27:2440-2447.
14. Extramiana F, Antzelevitch C. Amplified transmural dispersion of repolarization as the basis for arrhythmogenesis in a canine ventricular-wedge model of short-QT syndrome. *Circulation*. 2004;110:3661-3666.
15. Hondeghem LM. Thorough QT/QTc not so thorough: removes torsadogenic predictors from the T-wave, incriminates safe drugs, and misses profibrillatory drugs. *J Cardiovasc Electrophysiol*. 2006;

17:337-340.
16. Garberoglio L, Giustetto C, Wolpert C, Gaita F. Is acquired short QT due to digitalis intoxication responsible for malignant ventricular arrhythmias? *J Electrocardiol.* 2007;40:43-46.
17. Lu HR, Vlaminckx E, Hermans AN, Rohrbacher J, Van Ammel K, Towart R, Pugsley M, Gallacher DJ. Predicting drug-induced changes in QT interval and arrhythmias: QT-shortening drugs point to gaps in the ICHS7B Guidelines. *Br J Pharmacol.* 2008;154:1427-1438.
18. Aubert M, Osterwalder R, Wagner B, Parrilla I, Cavero I, Doessegger L, Ertel EA. Evaluation of the rabbit Purkinje fibre assay as an in vitro tool for assessing the risk of drug-induced torsades de pointes in humans. *Drug Saf.* 2006;29:237-254.
19. Food and Drug Administration, HHS. International Conference on Harmonisation; guidance on S7B Nonclinical Evaluation of the Potential for Delayed Ventricular Repolarization (QT Interval Prolongation) by Human Pharmaceuticals; availability. Notice. *Fed Regist.* 2005;70:61133-61134.
20. D'Alonzo AJ, Hess TA, Darbenzio RB, Sewter JC, Conder ML, McCullough JR. Effects of cromakalim or pinacidil on pacing- and ischemia-induced ventricular fibrillation in the anesthetized pig. *Basic Res Cardiol.* 1994;89:163-176.
21. D'Alonzo AJ, Zhu JL, Darbenzio RB, Dorso CR, Grover GJ. Proarrhythmic effects of pinacidil are partially mediated through enhancement of catecholamine release in isolated perfused guinea-pig hearts. *J Mol Cell Cardiol.* 1998;30:415-423.
22. Extramiana F, Antzelevitch C. Amplified transmural dispersion of repolarization as the basis for arrhythmogenesis in a canine ventricular-wedge model of short-QT syndrome. *Circulation.* 2004;110:3661-3666.
23. Hondeghem LM. Thorough QT/QTc not so thorough: removes torsadogenic predictors from the T-wave, incriminates safe drugs, and misses profibrillatory drugs. *J Cardiovasc Electrophysiol.* 2006;17:337-340.
24. Garberoglio L, Giustetto C, Wolpert C, Gaita F. Is acquired short QT due to digitalis intoxication responsible for malignant ventricular arrhythmias? *J Electrocardiol.* 2007;40:43-46.
25. Roden DM. Drug-induced prolongation of the QT interval. *N Engl J Med.* 2004;350:1013-1022.
26. Hondeghem LM, Carlsson L, Duker G. Instability and triangulation of the action potential predict serious proarrhythmia, but action potential duration prolongation is antiarrhythmic. *Circulation.* 2001;103:2004-2013.
27. Hondeghem LM. QT and TdP. QT: an unreliable predictor of proarrhythmia. *Acta Cardiol.* 2008;63:1-7.
28. Milberg P, Eckardt L, Bruns HJ, Biertz J, Ramtin S, Reinsch N, Fleischer D, Kirchhof P, Fabritz L, Breithardt G, Haverkamp W. Divergent proarrhythmic potential of macrolide antibiotics despite similar QT prolongation: fast phase 3 repolarization prevents early afterdepolarizations and torsade de pointes. *J Pharmacol Exp Ther.* 2002;303:218-225.
29. Lu HR, Vlaminckx E, Van Ammel K, De Clerck F. Drug-induced long QT in isolated rabbit Purkinje fibers: importance of action potential duration, triangulation and early afterdepolarizations. *Eur J Pharmacol.* 2002;452:183-192.
30. Champeroux P, Viaud K, El Amrani AI, Fowler JS, Martel E, Le Guennec JY, Richard S. Prediction of the risk of Torsade de Pointes using the model of isolated canine Purkinje fibres. *Br J Pharmacol.* 2005;144:376-385.
31. Guo D, Zhao X, Wu Y, Liu T, Kowey PR, Yan GX. L-type calcium current reactivation contributes to arrhythmogenesis associated with action potential triangulation. *J Cardiovasc Electrophysiol.* 2007;18:196-203.
32. Packer M, O'Connor CM, Ghali JK, Pressler ML, Carson PE, Belkin RN, Miller AB, Neuberg GW, Frid D, Wertheimer JH, Cropp AB, DeMets DL. Effect of amlodipine on morbidity and mortality in severe chronic heart failure. Prospective Randomized Amlodipine Survival Evaluation Study Group. *N Engl J Med.* 1996;335:1107-1114.
33. O'Connor CM, Carson PE, Miller AB, Pressler ML, Belkin RN, Neuberg GW, Frid DJ, Cropp AB, Anderson S, Wertheimer JH, DeMets DL. Effect of amlodipine on mode of death among patients with advanced heart failure in the PRAISE trial. Prospective Randomized Amlodipine Survival Evaluation. *Am J Cardiol.* 1998;82:881-887.
34. Udelson JE, DeAbate CA, Berk M, Neuberg G, Packer M, Vijay NK, Gorwitt J, Smith WB, Kukin ML, LeJemtel T, Levine TB, Konstam MA. Effects of amlodipine on exercise tolerance, quality of life, and left ventricular function in patients with heart failure from left ventricular systolic dysfunction. *Am Heart J.* 2000;139:503-510.
35. Littler WA, Sheridan DJ. Placebo controlled trial of felodipine in patients with mild to moderate heart failure. UK Study Group. *Br Heart J.* 1995;73:428-433.
36. Li K, Zhang X, Yuan YS, Zhao FL. A high-performance liquid chromatographic method for the determination of nicardipine in plasma and its application to pharmacokinetics in humans. *Biomed Chromatogr.* 1998;12:326-329.
37. Christensen HR, Antonsen K, Simonsen K, Lindekaer A, Bonde J, Angelo HR, Kampmann JP. Bioavailability and pharmacokinetics of isradipine after oral and intravenous administration: half-life shorter than expected? *Pharmacol Toxicol.* 2000;86:178-182.
38. Elliott HL, Meredith PA, Reid JL, Faulkner JK. A comparison of the disposition of single oral doses of amlodipine in young and elderly subjects. *J Cardiovasc Pharmacol.* 1988;12 Suppl 7:S64-66.
39. van Zwieten PA, Pfaffendorf M. Similarities and differences between calcium antagonists: pharmacological aspects. *J Hypertens Suppl.* 1993;11:S3-11.
40. Schoffstall JM, Spivey WH, Gambone LM, Shaw RP, Sit SP. Effects of calcium channel blocker overdose-induced toxicity in the conscious dog. *Ann Emerg Med.* 1991;20:1104-1108.
41. Lee SR, Noh SJ, Pronto JR, Jeong YJ, Kim HK, Song IS, Xu Z, Kwon HY, Kang SC, Sohn EH, Ko KS, Rhee BD, Kim N, Han J. The critical roles of zinc: beyond impact on myocardial signaling. *Korean J Physiol Pharmacol.* 2015;19:389-399.
42. Yun J, Bae H, Choi SE, Kim JH, Choi YW, Lim I, Lee CS, Lee MW, Ko JH, Seo SJ, Bang H. Taxifolin Glycoside Blocks Human ether-a-go-go Related Gene K^+ Channels. *Korean J Physiol Pharmacol.* 2013;17:37-42.